

Supplement for

**[Revisiting ocean carbon sequestration by direct injection:
A global carbon budget perspective]**

[Fabian Reith¹, David P. Keller¹, Andreas Oschlies¹]

[GEOMAR Helmholtz-Centre for Ocean Research Kiel,
Düsternbrooker Weg 20, 24105 Kiel, Germany]

Contents of this file

Table S1 to S2

Figure S1 to S5

Introduction

The supplement provides two tables showing the absolute DIC and PH values of the RCP 8.5 Control run at the injection sites and the respective changes in the WE simulations (section 3.2). Plus, the Figures S1 to S4 for section 3.4.2 that illustrate the explanation of the high correlation and apparent synchronicity in land carbon uptake between the WE simulations (Fig. 2 e) as well as Figure S5 that shows the deep convection related carbon uptake in the Southern Ocean in I-1500 (section 3.4.2).

Table S1: Absolute values of the DIC concentration near the injection sites at the end of the injection period (year 2119) of the RCP 8.5 Control run and comparison of absolute changes in the DIC concentration near the injection sites at the end of the injection period (year 2119) between Orr [2004] (Full range) and our WE simulations (WE simulations minus RCP 8.5 Control run).

| DIC [$\mu\text{mol/kg}^{-1}$] | Biscay | New York | Rio | Frisco | Tokyo | Jakarta | Mumbai |
|---|------------|------------|------------|------------|-----------|----------|------------|
| I-800 (RCP8.5) | 2246 | 2217 | 2249 | 2340 | 2301 | 2262 | 2307 |
| I-1500 (RCP8.5) | 2207 | 2195 | 2187 | 2361 | 2341 | 2272 | 2307 |
| I-3000 (RCP8.5) | 2184 | 2171 | 2186 | 2354 | 2338 | 2254 | 2287 |
| Δ DIC [$\mu\text{mol/kg}^{-1}$] | Biscay | New York | Rio | Frisco | Tokyo | Jakarta | Mumbai |
| Full range at 800m (Orr, 2004) | 261–1821 | 52 - 406 | 95 - 360 | 123 - 3178 | 58 - 271 | 79 -1095 | 159 - 1542 |
| I-800 | 357 | 307 | 187 | 356 | 111 | 211 | 232 |
| Full range at 1500m (Orr, 2004) | 143 - 4165 | 79 - 904 | 52 - 495 | 112 -1565 | 158 - 514 | 97 - 811 | 136 -1209 |
| I-1500 | 257 | 281 | 155 | 263 | 260 | 209 | 190 |
| Full range at 3000m (Orr, 2004) | 210 - 976 | 162 - 1222 | 109 - 1211 | 88 - 780 | 125 - 393 | 70 - 517 | 198 - 1966 |
| I-3000 | 299 | 463 | 245 | 215 | 265 | 175 | 199 |

Table S2: Absolute PH values near the injection sites at the end of the injection period (year 2119) of the RCP 8.5 Control run and comparison of absolute changes in PH near the injection sites at the end of the injection period (year 2119) between Orr [2004] (Full range) and our WE simulations (WE simulations minus RCP 8.5 Control run).

| PH | Biscay | New York | Rio | Frisco | Tokyo | Jakarta | Mumbai |
|------------------------------------|------------------|------------------|------------------|------------------|------------------|------------------|------------------|
| I-800 (RCP 8.5) | 7.78 | 7.84 | 7.74 | 7.55 | 7.72 | 7.80 | 7.68 |
| I-1500 (RCP 8.5) | 7.84 | 7.87 | 7.93 | 7.56 | 7.78 | 7.90 | 7.88 |
| I-3000 (RCP 8.5) | 7.97 | 7.98 | 7.97 | 7.86 | 7.88 | 7.93 | 7.95 |
| Δ PH | Biscay | New York | Rio | Frisco | Tokyo | Jakarta | Mumbai |
| Full range at 800m (Orr, 2004) | (-1.98) - (-.74) | (-1.08) – (-.12) | (-1.03) - (-.24) | (-2.43) - (-.29) | (-0.8) - (-.13) | (-1.8) - (-.17) | (-2.08) - (-.36) |
| I-800 | -.91 | -.85 | -.57 | -.74 | -.36 | -.64 | -.65 |
| Full range at 1500m (Orr, 2004) | (-2.34) - (-.39) | (-1.69) - (-.19) | (-1.29) - (-.12) | (-2.05) - (-.27) | (-1.3) - (-.036) | (-1.67) - (-.22) | (-1.78) - (-.3) |
| I-1500 | -.77 | -.83 | -.49 | -.72 | -.73 | -.68 | -.59 |
| Full range at 3000m (Orr, 2004) | (-1.7) - (-.65) | (-1.63) - (-.42) | (-1.77) - (-.25) | (-1.59) - (-.21) | (-1.09) - (-.33) | (-1.29) - (-.16) | (-2.02) - (-.54) |
| I-3000 | -.90 | -1.2 | -.77 | -.67 | -.78 | -.57 | -.53 |

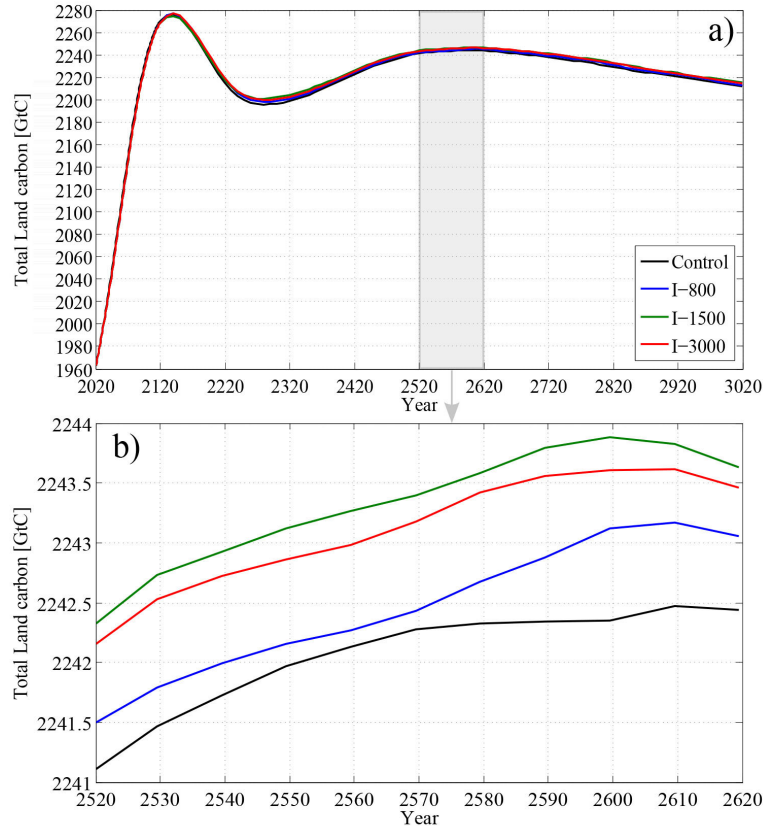


Figure S1: Total land carbon of the RCP 8.5 Control run and the WE simulations for (a) the whole simulation period and (b) the simulation period between the years 2520 and 2620.

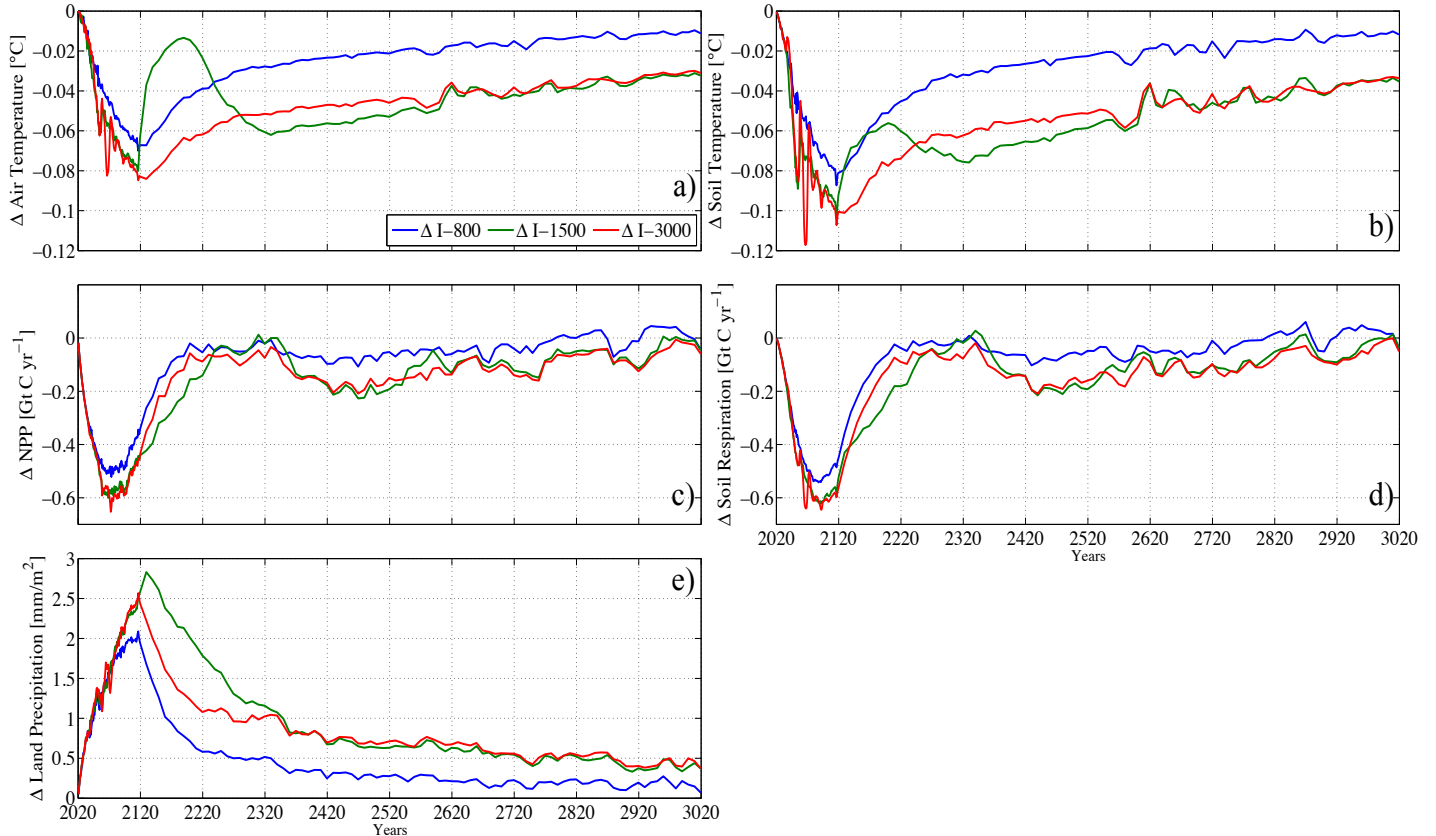


Figure S2: Absolute changes between the WE simulations and the RCP 8.5 control run for (a) global mean surface air temperature, (b) global mean soil temperature, (c) globally integrated net primary productivity on land, (d) globally integrated soil respiration, and (e) global mean precipitation over land

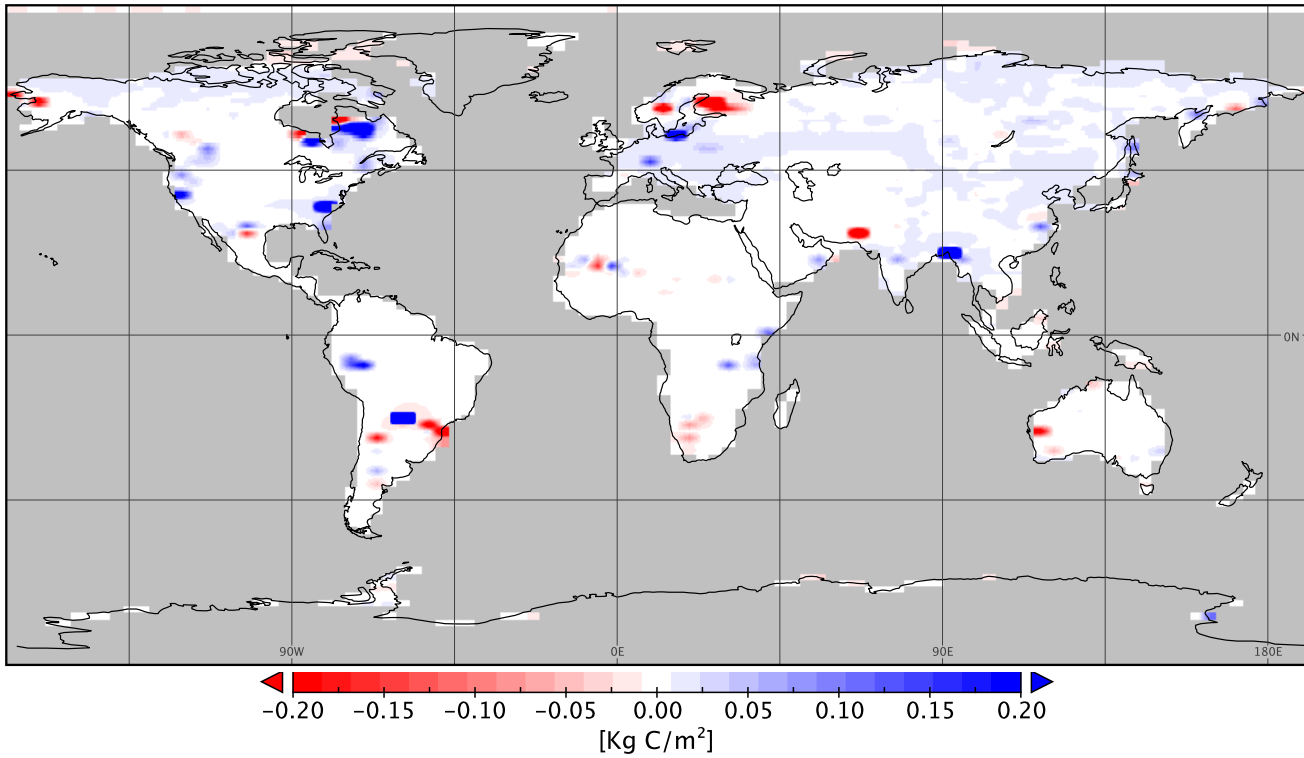


Figure S3: Absolute changes in land carbon between I-800 and the RCP 8.5 Control run for the synchronic increase illustrated in Figure 2 g, i.e., year 2600 minus 2570.

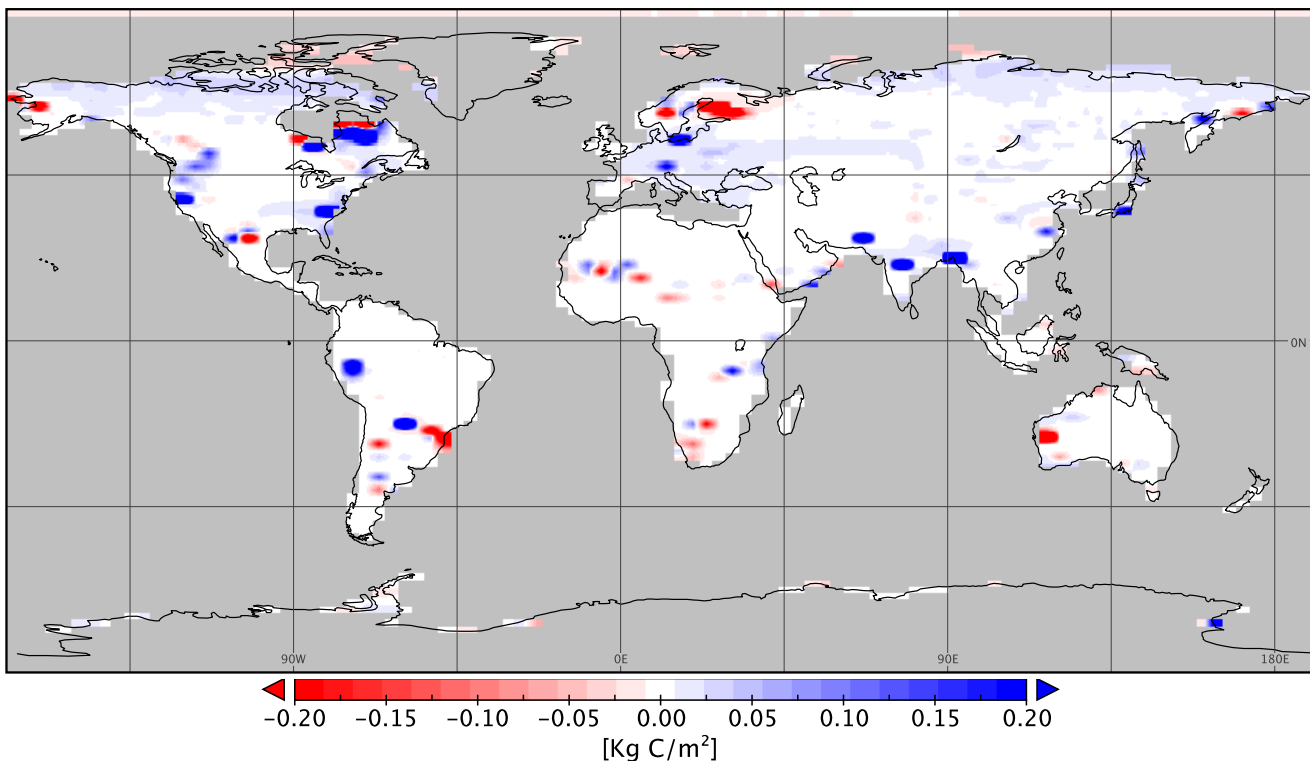


Figure S4: Absolute changes in land carbon between I-1500 and the RCP 8.5 Control run for the synchronic increase illustrated in Figure 2 g, i.e., year 2600 minus 2570.

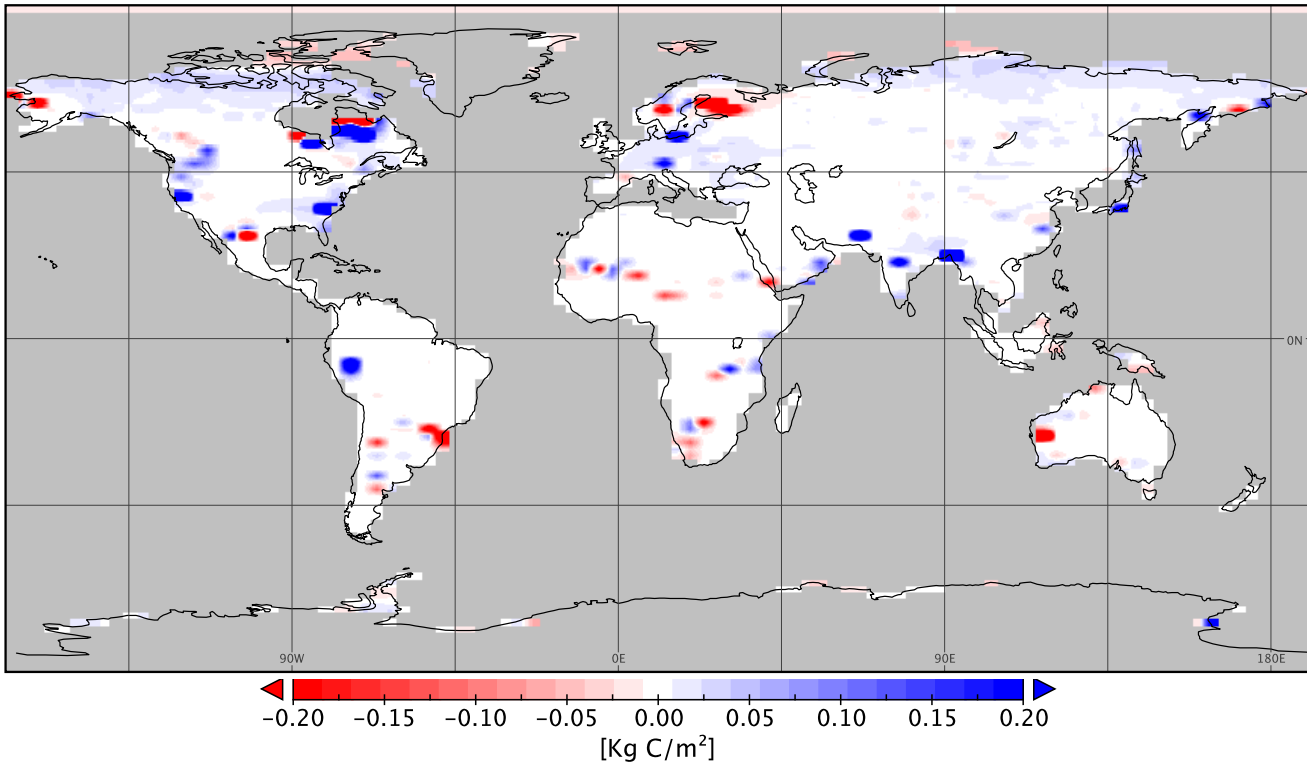


Figure S5: Absolute changes in land carbon between I-3000 and the RCP 8.5 Control run for the synchronic increase illustrated in Figure 2 g, i.e., year 2600 minus 2570.

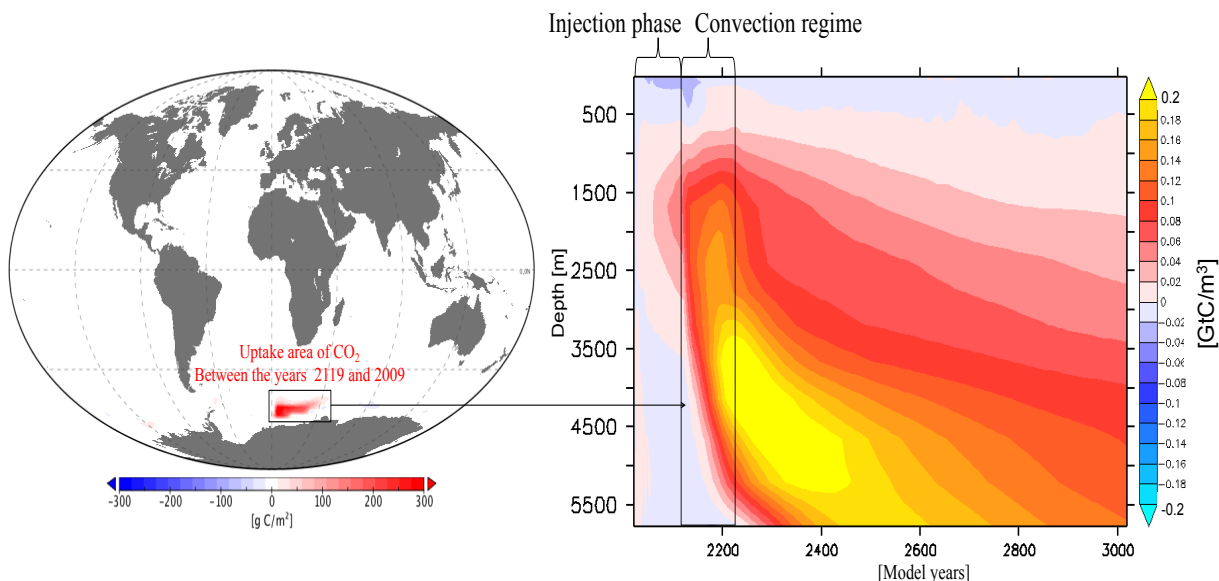


Figure S6: Downward carbon flux between the years 2119 and 2209 (I-1500 minus RCP 8.5 Control run) (left panel)
Absolute change in total oceanic carbon (I-1500 minus RCP 8.5 Control run) (right panel)